The suitability of discretized fluid equations to describe breakdown at atmospheric pressure

2005 J. Phys. A: Math. Gen. 38 6841

(http://iopscience.iop.org/0305-4470/38/30/016)

INSTITUTE OF PHYSICS PUBLISHING JOURNAL OF PHYSICS A: MATHEMATICAL AND GENERAL

J. Phys. A: Math. Gen. **38** (2005) 6841–6853 doi:10.1088/0305-4470/38/30/016

The suitability of discretized fluid equations to describe breakdown at atmospheric pressure

W N G Hitchon and C Wichaidit

Department of Electrical and Computer Engineering, University of Wisconsin, Madison, WI 53706, USA

E-mail: wichaidi@cae.wisc.edu

Received 4 April 2005
Published 13 July 2005
Online at stacks.iop.org/JPhysA/38/6841

Abstract

Discretized solutions of fluid equations can fail to accurately predict breakdown of a plasma for several reasons. During breakdown, the initial density can grow very rapidly indeed. As a consequence, small errors, such as those produced by 'numerical diffusion', can be greatly magnified. We present results which demonstrate the effect of numerical diffusion in the presence of strong growth in density over time, and we propose a criterion which indicates when a discretized solution of fluid equations can be expected to describe breakdown accurately. We further discuss how fluid schemes which employ energy conservation should be limited in the size of the discreteness parameters, i.e. mesh size and time step $(\Delta z, \Delta t)$, which can be employed. Unless $(\Delta z, \Delta t)$ are very small, the energy is not typically calculated accurately. (Schemes which do not conserve energy exhibit dramatic failures in accuracy, however.) Throughout this work, we compare the results of the various fluid models to a semi-analytic 'capacitor' model of breakdown. The time-dependent capacitor model (TDCM) avoids the major sources of error which can occur in fluid models. The TDCM agrees well with energy-conserving schemes, when those schemes employ very small $(\Delta z, \Delta t)$, whereas the TDCM can employ larger $(\Delta z, \Delta t)$, well beyond values at which most fluid models fail. Finally, we investigate a class of fluid models which attempts to capture the same physics as the TDCM, to study whether the TDCM is distinct from standard fluid models, and we suggest a fluid model which overcomes some of the limitations of a standard energy-conserving scheme.

PACS numbers: 02.70.−c, 52.25.−b, 51.50.+v, 52.65.−y, 52.80.−s

1. Introduction

In this paper we examine the steps which must be taken in order to specify a discretized fluid model which accurately describes breakdown at atmospheric or comparable pressure—which includes having the ability to capture the same physics as the time-dependent capacitor model (TDCM) of breakdown [1]. Modelling of breakdown in high-pressure discharges has often been performed using equilibrium fluid equations [2–9]. Guo *et al* [10, 11], Carman *et al* [12, 13] and others [14–16] have argued that it is necessary to use an energy-conserving scheme, and broadly speaking we strongly agree with them.

However, a number of restrictions on the discreteness parameters of mesh size and time step (Δz, Δt) arise in order to minimize the numerical diffusion as much as possible. The nature of these restrictions is one of the main issues addressed in this paper. Numerical diffusion, coupled with the very rapid growth in density with respect to time which occurs during breakdown, can present very significant challenges for developers of simulations. Some schemes exhibit no (or reduced) numerical diffusion, such as 'particle' simulation [25], Lagrangian schemes [26–28], and the TDCM [1]; these schemes tend to have advantages and disadvantages as compared to the discretized fluid equations which are more commonly used in this context. The convected scheme (CS) [18, 30] and the propagator approach to solving fluid equations [17] which is used here are Lagrangian schemes. They reduce numerical diffusion considerably, in some versions to a negligible level [29, 31], but nevertheless give rise to some numerical diffusion whenever fluid is mapped from one set of cells (or mesh) back onto another mesh.

The TDCM is a very simple physical model which represents the discharge as a number of capacitors, which in one dimension are in series, and uses energy conservation to calculate the density as these capacitors break down. These small capacitors are each considered to be uniform, and so each capacitor can be described analytically [19]. The TDCM has been successful in describing the essential physics obtained from a purely energy-conserving fluid scheme, which we denote the $R(\kappa)$ scheme [17]. The TDCM also has some distinct advantages over fluid schemes; for instance it has no numerical diffusion since the electrons are not usually allowed to move outside each capacitor. Electron transport between capacitors is permitted in the TDCM only in the first introduction of electrons in each capacitor; this first introduction can consist of 'injection' from a neighbour, so some transport is included. Another advantage of the TDCM is the ability to use a large mesh spacing Δz and a long time step Δt, which allows us to use 1000 times larger Δz and Δt than in the fluid–$R(\kappa)$ scheme, resulting in a much reduced computation time. The TDCM conserves energy and uses rates and transport coefficients found from the electric field (subject to energy conservation).

The $R(\kappa)$ scheme is not equivalent to the TDCM even though the results reported earlier agreed very well [1]. The $R(\kappa)$ scheme uses rates and transport parameters expressed as functions of mean kinetic energy, while the TDCM uses parameters found from the electric field. A relatively big time step cannot be applied to the $R(\kappa)$ scheme; if the time step is too large, the mean kinetic energy that a particle picks up in a time step will be artificially too high. The fraction of the energy which is put into ionization will then also be too high. This simple point, discussed in more detail later, appears to be overlooked in many cases. A similar limit applies to the mesh size (again, discussed below).

Here we also investigate a novel fluid scheme, using a propagator method that conserves density and energy, that uses rate parameters found from the electric field, and that allows us to use a relatively big time step by integrating the density in a moving cell with respect to energy gained within a time step; the significance of this is explained in section 2. This scheme ultimately reduces numerical diffusion considerably, but most importantly it allows us

to investigate the effects of numerical errors since the basic propagator scheme can function across a wide range of mesh sizes and time steps (not being limited by the Courant criterion).

We show that the 'best' such scheme, denoted as $R(E^\star)$, gives predictions which are as accurate as the $R(\kappa)$ scheme, but which are valid over a wider range of Δt. Indeed, in some cases the $R(\kappa)$ scheme may be difficult to use because of conflicting requirements on Δt. One of the main results of our investigation of these fluid models is that a novel limit on Δt arises in the presence of numerical diffusion coupled with exponentially growing density. The new limit on Δt is a lower limit, which may be difficult to reconcile with the limits which apply to some schemes, since the other limits on Δt are upper limits.

On a short time scale, the 'equilibrium' fluid scheme, which we denote as the $R(E)$ scheme, which does not conserve energy and uses parameters found solely from the electric field, shows fair agreement with the $R(\kappa)$ scheme and our kinetic model [17]. The $R(E)$ scheme seems to get the correct values of the rates and transport coefficients over a short amount of time. Unfortunately, when the electric field saturates, i.e. over a long period of time as the discharge settles down, the $R(E)$ scheme shows an unphysical growth of density, even in regions where density is energetically not allowed. Whereas the $R(E^\star)$ and $R(\kappa)$ schemes do not readily obtain the exact same values of α (the fraction of the energy that goes into ionization as opposed to vibrational and rotational excitations or other inelastic processes), they give good agreement for the overall density after breakdown, because they both conserve energy.

In order to get the $R(E^\star)$ and $R(\kappa)$ schemes to agree well over a range of mesh spacings Δz and time steps Δt, there are various limitations on the time step, which we discuss in section 4. Some of the limits are well known, such as the Courant limits, but some of them are not. Some of them only apply to energy-conserving schemes of a certain kind: $R(\kappa)$. However, a new lower limit on the time step is derived, which is needed to prevent significant errors due to the combination of numerical diffusion and rapid growth in density. This new limit applies to any fluid model which employs a mesh to describe transport in the presence of an exponential density growth during particle movement. The TDCM is not limited as to its time step in this regard, since transport between 'cells' is only permitted in a limited sense in the TDCM, and numerical diffusion is essentially absent. The TDCM is only limited by the dielectric relaxation time, and as such is useful for comparison to the various more standard fluid models.

The next section describes the numerical implementation of the fluid models employed here, including a novel propagator scheme (which we denote as $R(E^\star)$). Section 3 briefly outlines the physics contained in the models. Much of this paper is concerned with the speed at which the ionization front travels. The front travels because of electron drifts and artificial movement of the front caused by numerical diffusion. The role of photoionization and how it can be readily included in the TDCM are also discussed. Then, section 4 describes the limits which can apply to the time step: the well-known Courant limits, in the case of finite difference schemes; the dielectric relaxation time, which is a physically relevant time scale which must be resolved; and two new limits, one which is needed to minimize the effects of numerical diffusion in the presence of density strongly increasing over time, and one which is needed for accurate calculation of rates in an energy-conserving scheme. Section 5 illustrates the effects of the choice of Δt using numerical results, and section 6 is the conclusion.

2. Numerical implementation of fluid models of breakdown

In the present work, fluid models using propagators [17] have been used throughout. The 'standard' energy-conserving version is denoted as $R(\kappa)$. In the $R(\kappa)$ scheme, rates are all

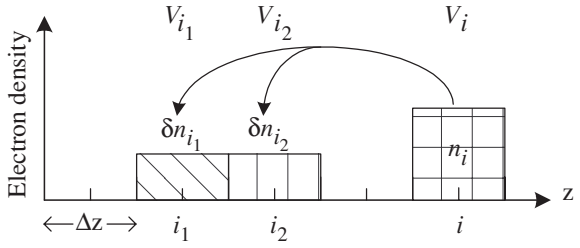

Figure 1. Density n initially in cell i with voltage V_i is moved and densities δn_{i_1} and δn_{i_2} are put back in cells i_1 and i_2 associated with voltages V_{i_1} and V_{i_2} respectively.

calculated using the kinetic energy κ. The $R(\kappa)$ model has also been extended to use rates and transport coefficients found from the electric field (as in an 'equilibrium' model, such as the $R(E)$ scheme), and at the same time to conserve energy (as in the $R(\kappa)$ scheme) in a new model which we denote as the $R(E^\star)$ scheme. The purpose of developing this new scheme is to study whether a fluid model could be set up which can capture the same physics as the TDCM, and if so, to examine its performance.

In this section we describe the basic physics which is common to all the schemes we consider. We then outline the types of numerical scheme we employ. The basic elements of the scheme we propose are illustrated in figure 1. Particles with initial mean kinetic energy κ_i and potential energy V_i, in initial cell i, move due to drift and diffusion to final cells i_1 and i_2 (more than two final cells are likely to arise, but need not be shown here) with potential energies V_{i_1} and V_{i_2}. The numbers put in each cell are found from an overlap rule, based on the motion of the particles in the cell as they drift and diffuse, as described in [18, 19]. The particles are put back in i_1 in such a way as to conserve energy. In the $R(\kappa)$ scheme, the kinetic energy in i_1 (say) is simply updated to allow for the energy brought in by the new particles, and energy is subsequently taken out during inelastic processes, at a rate depending only on κ in cell i_1.

In the $R(E^\star)$ scheme, particles are put back in cell i_1 with mean kinetic energy $\kappa\left(E_{i_1}\right)$, where E_{i_1} is the electric field in cell i_1, and $\kappa\left(E_{i_1}\right)$ is the equilibrium mean kinetic energy in an electric field E_{i_1}. Any excess mean kinetic energy above $\kappa\left(E_{i_1}\right)$ which electrons pick up in the move from i to i_1 is used in inelastic processes—see below. The number of electrons δn_{i_1}, which are put back in i_1, thus add a kinetic energy $\delta n_{i_1}\kappa\left(E_{i_1}\right)$ to the total kinetic energy in that cell. Conservation of energy is handled similarly to the $R(\kappa)$ scheme [17]. In each cell i of the mesh, the total number of particles in the cell, n_i, and the total kinetic energy κ_i^{TOT} are stored (as well as the voltage V_i). In this procedure, therefore, the total kinetic energy κ_i^{TOT} increased by $\delta n_{i_1}\kappa\left(E_{i_1}\right)$, and the number increased by δn_{i_1}.

In this discussion of the $R(E^\star)$ scheme, we have assumed that the final cells have a lower potential energy for the particles than the initial cell, and if this is the case and excess kinetic energy is available, we assume excitation and ionization took place during the move. The number of particles in the initial cell is divided into fractions going to each final cell according to an overlap rule [18]. Let the number starting from i going to i_1 (i.e. the number which would go from i to i_1 in the absence of ionization) be n_{i,i_1}. Then the number which reach i_1 from i will be

$$\delta n_{i_1} = n_{i,i_1}\exp(\alpha\mathcal{E}/\mathcal{E}_{\mathrm{Iz}}). \tag{1}$$

$\mathcal{E}_{\mathrm{Iz}}$ is the ionization potential. $\alpha \equiv \alpha(E)$ is the fraction of the energy $\mathcal{E}$ which goes into ionization, and α allows for energy loss to vibration, excitation, etc, since the rest of the

energy goes into other inelastic processes [19]. $\mathcal{E}$ is the energy per particle available for inelastic processes,

$$\mathcal{E} = \kappa_i - \kappa\left(E_{i_1}\right) + q\left(V_i - V_{i_1}\right). \tag{2}$$

q is the particle charge. The expression for δn_{i_1} is the result of integrating the equation

$$\frac{\mathrm{d}n}{\mathrm{d}\mathcal{E}} = \frac{\alpha}{\mathcal{E}_{\mathrm{Iz}}} n \tag{3}$$

over the particle motion, and is preferable to numerically integrating equation (3), once per numerical step, since it allows a considerably larger step. (If equation (1) is not employed, another upper limit on Δt arises.)

If the final cells are at a higher potential energy than the initial cells, we do not allow ionization, and we only allow motion to those cells if κ_i in the initial cell is high enough to overcome the potential difference $W = q\left(V_{i_1} - V_i\right)$. The particles are then put back in cell i_1, each bringing with them a kinetic energy of $\kappa_i - W$.

We also tested a scheme where $\kappa_i =$ constant, so $\mathcal{E} = q\left(V_i - V_{i_1}\right)$. This does not conserve energy when particles move upstream, but shows somewhat less upstream diffusion than was observed in the fluid–$R(E)$ scheme (that is, the 'equilibrium' fluid model). To be consistent with the TDCM, in the $R(E^\star)$ scheme, the mobility, diffusion coefficient, ionization rate and fraction of the energy which goes to ionization, $(\mu, D, I_{\mathrm{Iz}}, \alpha)$, are to be found from E. In the $R(\kappa)$ scheme these quantities are instead found from κ, and κ in each cell is found from conservation of energy [17].

3. Physical model

Transport parameters and the ionization rate (calculated using α, the fraction of the energy used in inelastic processes which goes into ionization) that are used in the model are found from kinetic simulations. Details are given elsewhere [17, 19]. We emphasize that the use of α does properly include the known inelastic processes. It is well known that nitrogen metastable molecules are produced very efficiently; an estimate in [19] predicted that the number of metastable molecules could not reach a significant level within one breakdown cycle. Although the role of photoionization is somewhat unclear, the physical picture we propose of breakdown does not require great accuracy as to the level of photoionization. It requires somewhat more accuracy as to the spatial range of the photons creating the ionization. The role of photoionization in streamer discharges has been studied numerically and experimentally [21–24]. For the N_2 discharge studied here the ratio of the number of photoions to ions produced by electron impact, ψ (described in [21]) $\lesssim 10^{-8}$. It is difficult to justify including such a low level of ionization while neglecting other sources. If we do include the photoionization, we find that at a typical growth rate of $\gamma \sim 4 \times 10^9$ s^{-1}, a relative density of 10^{-8} can grow to unity in time $\tau_{\mathrm{gr}} = \frac{1}{\gamma} \ln(10^8) \sim 6 \times 10^{-9}$ s. The range of the radiation for these conditions is $l_a \lesssim 10^{-4}$ m [23], so the 'speed' of propagation by this mechanism is limited to $l_a/\tau_{\mathrm{gr}} \sim 2 \times 10^4$ m s^{-1}. The velocity of the front due to photoionization appears to be considerably smaller than the electron drift velocity, $v_{\mathrm{dr}} \sim 1$–6×10^5 m s^{-1}, for these conditions. In the cases we have examined, the speed of spreading of the front due to ionization is not likely to exceed that of the 'injection' [1] we have already included, except in the upstream direction where the densities produced are very low. Photoionization can be readily included by injection in the TDCM, but the time scale of the photoionization in our case is too large compared to the breakdown time. Since the speed of propagation by photoionization is approximately 2×10^4 m s^{-1}, and the mesh size is 2.25×10^{-4} m, then the injection for

this mechanism should be applied at time ∼11 ns, this being the time for photoionization to advance the front across one cell of the mesh; whereas the breakdown time is approximately 5 ns. Downstream, therefore, it will have little effect. Upstream, it can introduce some ionization where otherwise there would be none. The new electrons then promptly drift downstream, however, and the density produced is again very small. The main effect may be to spread the streamer sideways—at an angle which is roughly the photoionization spreading speed divided by the electron drift velocity. This is again small—and cannot be included in the 1D models discussed here.

4. Limits on the time step

As our fluid models use a propagator method [17], they are not restricted by the Courant criteria and can be used over a relatively wide range of Δz and Δt. The physical and to some extent numerical aspects of the problem place additional limitations on the discreteness parameters, however. We have examined the limitations on the time step to find the range where the fluid–$R(E^\star)$ and $R(\kappa)$ are valid, and run the models to see how well they agree for various Δz and Δt. In this section we outline the limits which apply, starting with the Courant (or Courant–Fredrichs–Levy), τ_{CFL} and $\tau_{\mathrm{CFL-D}}$ limits for drift and diffusive transport, respectively, on a finite difference scheme. Next, we mention the dielectric relaxation time τ_{diel}, which is a crucial physical time scale which must be resolved (i.e. $\Delta t \ll \tau_{\mathrm{diel}}$) for accuracy and stability. We then derive a new lower limit on Δt, for a situation where numerical diffusion occurs in the presence of (exponential) time growth in density, denoted as τ_{NE}. We discuss the limits which can arise in a simple energy-conserving scheme. Finally, we illustrate the role of these limits in determining the accuracy of simulations in the next section.

4.1. Courant limits

In a general finite difference (FD) scheme, there are limits on the discretization, usually expressed as limits on the time step, which must be obeyed for accuracy, and sometimes for stability. In a system with a characteristic velocity v, it is necessary that the ratio, c, of the physical velocity, v, to the velocity of 'numerical propagation', $\Delta z/\Delta t$, obeys

$$c = \frac{v\Delta t}{\Delta z} \ll 1. \tag{4}$$

In the presence of diffusion, with diffusion coefficient D, it is additionally required that

$$d = \frac{D\Delta t}{(\Delta z)^2} \ll 1. \tag{5}$$

Thus, from equation (4), the Courant time limit (τ_{CFL}) is

$$\tau_{\mathrm{CFL}} = \frac{\Delta z}{v}, \tag{6}$$

and from equation (5), the Courant diffusion limit ($\tau_{\mathrm{CFL-D}}$) is

$$\tau_{\mathrm{CFL-D}} = \frac{(\Delta z)^2}{2D}. \tag{7}$$

Any time step that is employed in a FD scheme has to obey

$$\Delta t \ll \tau_{\mathrm{CFL}}, \tau_{\mathrm{CFL-D}}, \tag{8}$$

for accuracy in describing time evolution, and some instances in stability.

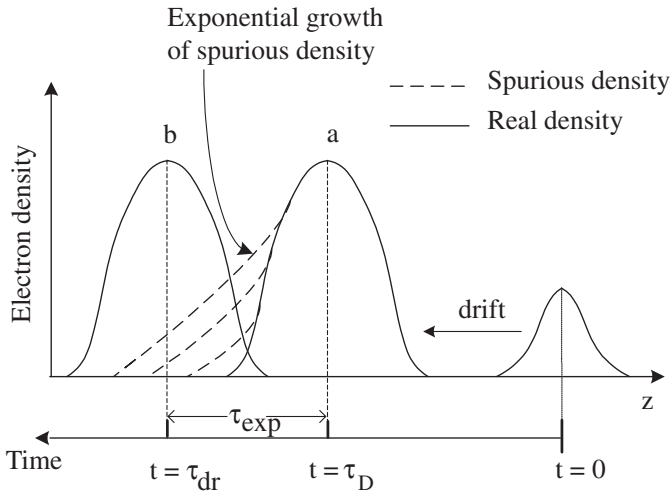

Figure 2. Schematic illustrates (1) a density pulse which starts at time $t = 0$ and drifts to position a, at the same time as spurious diffusion takes place (dashed lines), both before $t = \tau_D$. (2) Exponential growth of the spurious density takes place after $t = \tau_D$, for a time $\tau_{\rm exp}$. The real density moves from position a to position b in the same time $\tau_{\rm exp}$, thus the real density moves from its initial position to position b in a total time $\tau_{\rm dr} = \tau_D + \tau_{\rm exp}$.

4.2. Dielectric relaxation time ($\tau_{\rm diel}$)

The dielectric relaxation time $\tau_{\rm diel}$ is the time scale of the decay of excess charge, in a collisional fluid model, given by

$$\tau_{\rm diel} = \frac{\epsilon_0}{q\mu n_e}. \tag{9}$$

ϵ_0 is the permittivity of free space, μ is the mobility of electrons and n_e is the electron density. Thus if the numerical scheme is to describe the evolution of the electric field, the time step should obey

$$\Delta t \ll \tau_{\rm diel}. \tag{10}$$

4.3. Numerical diffusion and exponential growth limit ($\tau_{\rm NE}$)

In this section we consider a situation where a flowing fluid is growing exponentially in density over time. We are concerned to find whether numerical diffusion can artificially introduce 'spurious' density to a region, and that density subsequently grows exponentially until it reaches a value comparable to the actual density, which arrives later. The 'spurious' density is assumed to be in a region with a higher growth rate than the peak of the actual density, whose growth is ignored, for now. We thus consider numerical diffusion for a time τ_D which delivers spurious density a distance z downstream. The spurious density then undergoes exponential growth for a time $\tau_{\rm exp}$. In the same total time, $\tau_{\rm dr}$ as taken by the combined diffusion and growth, the actual density drifts the distance z (as shown in figure 2), where

$$\tau_{\rm dr} = \frac{z}{\mu E}, \tag{11}$$

and where

$$\tau_{\rm dr} = \tau_D + \tau_{\rm exp}. \tag{12}$$

Then the (normalized) spurious density, n_s, which is obtained from the diffusion followed by the exponential growth, is

$$n_s = \exp\left(\frac{-z^2}{2D_n\tau_D}\right)\exp(\gamma\tau_{\rm exp}), \tag{13}$$

where γ is the growth rate and $D_n = \frac{(\Delta z)^2}{2\Delta t}$ is the numerical diffusion coefficient. This reaches a 'critical' value (rivalling the 'real' density) when n_s equals 1, in which case

$$\frac{z^2}{2D_n\gamma} = \tau_D\tau_{\rm exp} = \tau_D(\tau_{\rm dr} - \tau_D), \tag{14}$$

and the biggest value that the rhs of equation (14) can attain is $\tau_{\rm dr}^2/4$. Substituting the value of $\tau_{\rm dr}$ from equation (11) yields the value of the time step when equality is reached (that is, when the 'spurious' density is as large as the real density);

$$\tau_{\rm NE} = \frac{1}{4}\frac{(\Delta z)^2\gamma}{v_{\rm dr}^2}, \tag{15}$$

where the drift velocity $v_{\rm dr} = \mu E$.

Another point of view on this process allows for the fact that the code is energy conserving, so the particle density only grows when particles move and gain kinetic energy. If the electric field E is roughly constant, then the density grows as a cell moves, in proportion to

$$\exp\left(\frac{\alpha q E z}{\mathcal{E}_{\rm Iz}}\right). \tag{16}$$

However, the motion in this case is assumed to be caused in part by numerical diffusion, and the numerical diffusion makes the density vary with space, according to

$$\exp\left(\frac{-z^2}{2D_n t}\right). \tag{17}$$

The overall spurious density is given (approximately) by the product of these.

If this product approaches unity, then the spurious density might approach the 'real' density. To simplify matters, suppose we are considering a 'typical' distance the particles would travel in the course of the simulation. In that case, $z \sim v_{\rm dr}t$, and the combined exponents are

$$c = \alpha q\frac{Ez}{\mathcal{E}_{\rm Iz}} - \frac{z^2}{2D_n t} \tag{18}$$

$$\sim z\left(\alpha\frac{qE}{\mathcal{E}_{\rm Iz}} - \frac{v_{\rm dr}}{2D_n}\right). \tag{19}$$

If $c = 0$, which occurs when the (normalized) 'spurious' density reaches unity, then

$$\frac{\alpha eE}{\mathcal{E}_{\rm Iz}} = \frac{v_{\rm dr}}{qD_n}. \tag{20}$$

Now in equation (16), if $z = v_{\rm dr}t$ we obtain a variation like $\exp(\gamma t)$, where $\gamma = \alpha q v_{\rm dr}E/\mathcal{E}_{\rm Iz}$, so equation (20) yields $v_{\rm dr}^2/\gamma = D_n$. Using $D_n = \frac{(\Delta z)^2}{2\Delta t}$ we obtain the limiting time step

$$\tau_{\rm NE} = \frac{\gamma}{v_{\rm dr}^2}(\Delta z)^2, \tag{21}$$

which except for a numerical factor is the same expression as equation (15). For accuracy, meaning for the spurious density resulting from numerical diffusion to be small, the time step must obey

$$\Delta t \geqslant \tau_{\rm NE}. \tag{22}$$

This is a lower limit on the time step—but since it essentially expresses the need for modest numerical diffusion, this is not surprising. Of course, the lower limit can be reduced by decreasing Δz, the mesh size.

4.4. Energy-conserving scheme time limit (τ_κ)

We now outline limits on the discreteness parameters which apply to an energy-conserving scheme. In a purely energy-conserving scheme (such as the fluid–$R(\kappa)$), the mean kinetic energy of electrons is a primary-dependent variable. It would be unphysical if the time step was so big that electrons could gain a great deal of kinetic energy in a time step. For example, if the mean energy was 2 eV, and the distance that electrons moved in Δt allowed them to pick up 5 eV in the step, then the extra amount gained would lead to an overestimate of the mean energy. If shorter steps were used, the electrons might pick up 0.1 eV at each step, which would not lead to a major overestimate of the mean energy. They would lose much of that energy to inelastic processes, at each step. In other words, if the mean energy is 2 eV, it might be acceptable for the energy to fluctuate by 0.1 eV per step. Fluctuations of 5 eV would not be acceptable. If the time step were too large, the mean energy of the electrons would tend to be overestimated, and that energy, when used in inelastic processes, would tend to create too many new electrons because at high 'temperature' a larger fraction of the available energy goes into ionization, as opposed to other inelastic processes. Similarly, if the mesh size is large, the electrons will also travel 'far' as they move from one cell to the next, gaining too much energy in the step, in the same sense as explained above. The distance that an electron can travel should be much less than δz_κ, the ratio of its mean kinetic energy κ and the electric field force on the particle, qE,

$$\delta z_\kappa = \frac{\kappa}{qE}. \tag{23}$$

Thus the spatial mesh size Δz should be much less than δz_κ to prevent an excessive gain in kinetic energy. Similarly, in a time step a particle can travel a distance $v_{\rm dr}\Delta t$ which should be also much less than δz_κ. Thus the time step in this $R(\kappa)$ scheme is limited by

$$\Delta t \ll \tau_k = \frac{\delta z_\kappa}{v_{\rm dr}}. \tag{24}$$

For instance, the field strength in our calculations using the $R(\kappa)$ model is approximately 1.7 V/Δz. The energy limitation discussed here, that only applies to the $R(\kappa)$ model, means that a particle should not gain kinetic energy comparable to mean kinetic energy κ 5 eV in a time step. The spatial mesh size must also be small enough that electrons cannot pick up more energy than a fraction of 5 eV. Therefore, as reported in [17], it is necessary to use very fine Δz ($\sim 2.5 \times 10^{-7}$ m) and Δt ($\sim 5.0 \times 10^{-14}$ s) to obtain accuracy in the fluid–$R(\kappa)$ scheme.

The role of these time-step limits is illustrated in section 5.

5. Numerical results

In this section we perform, first, a series of simulations with the fluid–$R(E^\star)$ scheme and study the effect of variation in Δz and Δt in the light of the various limitations on the time step. We then compare the results obtained from the TDCM, the fluid–$R(\kappa)$, and the $R(E^\star)$ schemes. The simulations were performed for a 5 mm air gap between two 1.5 cm dielectric slabs ($\epsilon_r \sim 3$) in N_2 at atmospheric pressure with 100 kV direct applied voltage.

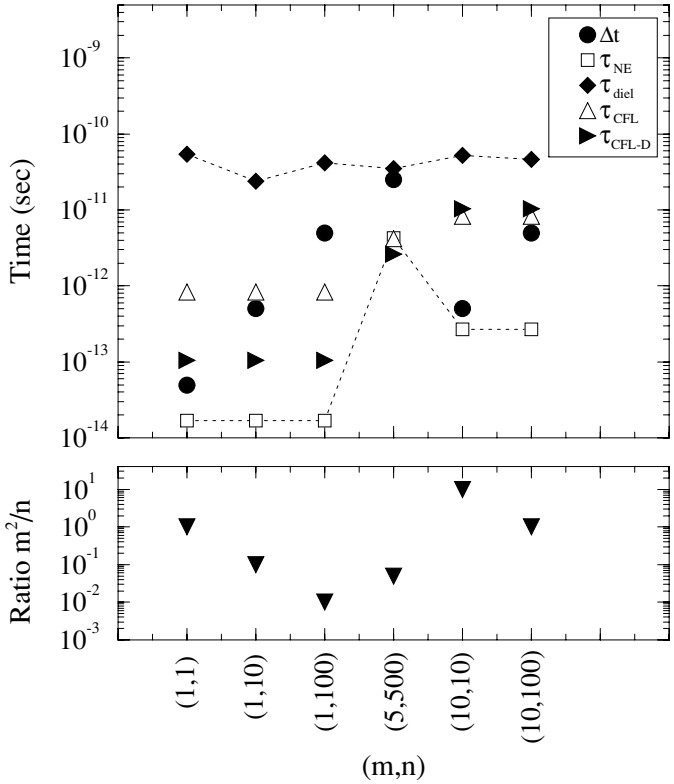

Figure 3. Constraint on Δt, for different Δz. Some choices of m and n (where $\Delta z = m\Delta z'$ and $\Delta t = n\Delta t'$) with their corresponding time steps (Δt); the ratio $\frac{m^2}{n}$, $\tau_{\rm CFL}$, $\tau_{\rm CFL-D}$, $\tau_{\rm NE}$ and $\tau_{\rm diel}$ are also shown. The actual time step Δt is required to lie below $\tau_{\rm diel}$ and above $\tau_{\rm NE}$. The Courant limits do not apply to the propagator scheme used here, but are shown for reference. Values of Δt which approach the upper limit may lead to inaccuracy or instability. Near the lower limit, spurious downstream density is observed.

5.1. Mesh size (Δz) and time step (Δt) in the fluid–$R(E^\star)$ model

We have explored and compared fluid runs with mesh sizes/time steps of $\Delta z = m\Delta z'$ and $\Delta t = n\Delta t'$ by varying m and n where m and n are integers. Thus, the numerical diffusion coefficient D_n is defined as

$$D_n = \frac{(m\Delta z')^2}{2(n\Delta t')}. \tag{25}$$

The choice of m and n that gives the lowest D_n will give the least numerical diffusion.

Some choices of Δz and Δt and the corresponding limits on the allowed time step are shown in figure 3. In this figure we show choices of Δz and Δt such that the fluid–$R(E^\star)$ works relatively well. (The $R(\kappa)$ scheme works accurately only for $m = n = 1$ for reasons discussed in section 4.4.) We use $\Delta z' = 2.5 \times 10^{-7}$ m and $\Delta t' = 5.0 \times 10^{-14}$ s as the base case. Δt must lie between $\tau_{\rm diel}$ (upper limit) and $\tau_{\rm NE}$ (lower limit) in a discretized fluid scheme. The propagator scheme is not restricted by the two Courant limits ($\tau_{\rm CFL}$ and $\tau_{\rm CFL-D}$), however. If we use $\Delta t \sim \tau_{\rm NE}$, the exponential growth of the spurious density will significantly distort the results. The 'physical' density will have to compete with the artificial density which grows downstream—see the case $n = 10$, $m = 10$, in figure 4(*b*).

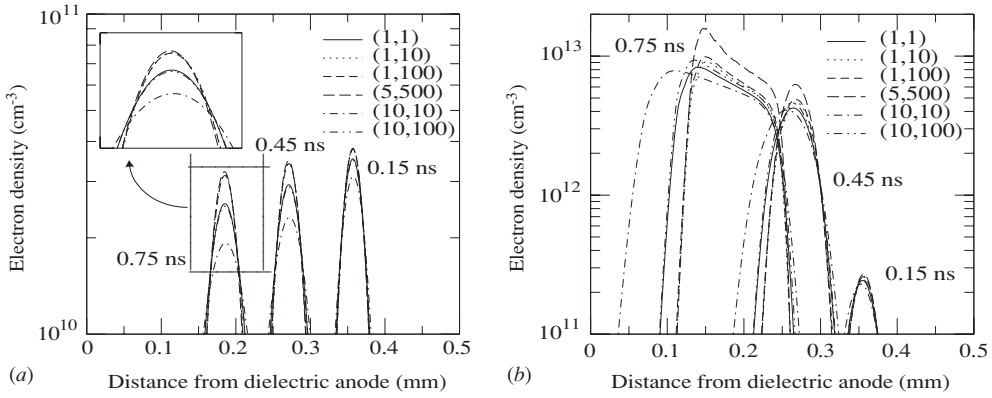

Figure 4. Time evolution of electron densities calculated from the fluid–$R(E^\star)$, for various (m, n). (a) Without ionization, the propagator method predicts the drift velocity correctly. The density depends on the numerical diffusion, which is small provided $D_n = \frac{(\Delta z)^2}{2\Delta t} \propto \frac{m^2}{n}$ is small enough. (b) With ionization, the case (10,10) violates $\Delta t > \tau_{\rm NE}$, and the front accelerates artificially due to numerical diffusion plus density growth. (5, 500) violates $\Delta t < \tau_{\rm diel}$.

In the discharge we consider, the fluid–$R(E^\star)$ is used to study the effects of variations in Δz and Δt. Plots of electron density without and with ionization are shown in figures 4(a) and (b) respectively. The time evolution is taken at 0.15, 0.45 and 0.75 ns.

In the absence of ionization (figure 4(a)), the $R(E^\star)$ obtains the correct speed for all choices of (m, n). Nevertheless, the magnitude of the density separates the plots into three groups. When $m = n = 10$, the result obtained is the lowest in magnitude. In this case, the time step used has the highest ratio of $\frac{m^2}{n}$ $(= 10)$—which means that the result obtained by using $m = n = 10$ suffers from distortion by numerical diffusion. The ratio $\frac{m^2}{n}$ determines the difference between the various groups. In the middle group $((m, n) = (1, 1), (10, 100))$ so $\frac{m^2}{n} = 1$ and in the highest group $((m, n) = (1, 10), (1, 100), (5, 500))$ so $\frac{m^2}{n} \ll 1$.

When the ionization process is present, the effect of the sizes of Δz and Δt can be seen more dramatically. It is now clear that when $m = n = 10$, and $\Delta t \sim 2\tau_{\rm NE}$, the electron density shows the effect of spurious density discussed above, that is, the ionization front accelerates artificially. In the case $(m, n) = (5, 500)$, the time step is very close to the value of $\tau_{\rm diel}$, so accuracy and stability are not guaranteed (see figure 4(b)), and we obtain a density which is too high.

5.2. The comparison of breakdown simulation using the fluid models and the TDCM

To further compare the performance of the numerical models we have developed, the fluid–$R(\kappa)$, $R(E^\star)$ schemes and the TDCM were used to simulate a 5.0 mm discharge in nitrogen gas between two 1.5 cm dielectric slabs. The electron density from the proposed numerical models after the total breakdown time of approximately 5 ns is shown in figure 5.

The $R(\kappa)$ and $R(E^\star)$ models and the TDCM agree satisfactorily[1], provided they employ equivalent values of α. Since the fluid models call for α to be expressed in terms of κ and E, respectively, this agreement is not automatic. They share the advantage of being energy

[1] By comparing the mean kinetic energy of electrons, κ, obtained from the CS and the fluid–$R(\kappa)$ scheme, it was found that the κ value from the $R(\kappa)$ scheme is approximately 10% less than that from the CS. Thus $\kappa' = 1.1\kappa$ is used in obtaining the ionization parameters (α and the ionization rate) in the fluid–$R(\kappa)$ scheme.

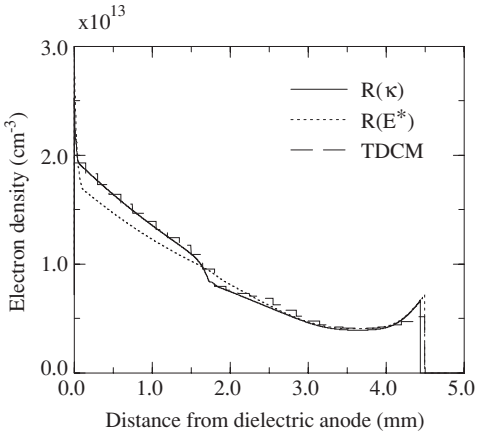

Figure 5. Final electron density calculated from the fluid–$R(\kappa)$, $R(E^\star)$ schemes and the TDCM (initialized with a Gaussian-shaped density).

conserving, however, so they produce results for the 'final' density which agree with each other as well as α allows. The $R(\kappa)$ and the $R(E^\star)$ schemes show a slight difference at the upstream edge. The equilibrium $R(E)$ scheme (not shown) does not conserve energy, so in a long run, it produces an unphysical exponential density growth, including growth in the area where the electrons are energetically prohibited.

When $m = 1000$ and $n = 100$ ($\Delta t = 5 \times 10^{-12} \approx 0.1\tau_{\text{diel}}$), Δz and Δt are equal to the mesh spacing and time-step size (respectively) used in the TDCM; the fluid–$R(E^\star)$ went unstable. This demonstrates one advantage of the TDCM over fluid models—it is free of numerical diffusion and has the ability to work with a relatively coarse spatial mesh and very large time step.

In these simulations the Debye length is always at least three elastic mean free paths, and usually a great deal more. As a result, in some locations, the equilibrium approximation to the transport coefficients is starting to break down. It might be argued that some other fluid model would be more applicable, such as the fluid–$R(\kappa)$ model or that in [20]. In fact, only a kinetic model is truly suited to describe these regions. However, comparison of the $R(E^\star)$ and the $R(\kappa)$ schemes suggests that in the region where the electric field changes rapidly the two models agree very closely as to the values of the transport coefficients.

Comparison to the kinetic code indicates that all of the fluid codes perform as well as each other for short times. The non-energy-conserving code, of course, fails at longer times.

6. Conclusions

We have examined the limitations on the discreteness parameters (Δz, Δt) employed in implementing a fluid model of breakdown at 'high' gas pressures ($\sim$1 atmosphere). We also examined a class of models which captures the same physics as the time-dependent capacitor model of discharge breakdown. Perhaps surprisingly, the TDCM performs somewhat better than the fluid models, in two regards. The TDCM is not subject to numerical diffusion, as opposed to those fluid models which use a discrete mesh. The TDCM is also less susceptible to numerical instabilities associated with the time step approaching the dielectric relaxation time. (The disadvantage of the TDCM is that the price of removing numerical diffusion was the introduction of an 'injection' mechanism [1] which seeds breakdown, which might introduce

inaccuracy but which in practice is probably less of a problem than numerical diffusion.) A new expression for a minimum permissible time step τ_{NE} was derived, which is needed to avoid serious errors due to the combination of numerical diffusion and density growing rapidly over time.

The fluid model we developed nevertheless works considerably better than a purely energy-conserving scheme. The latter is required to use very small values of the discreteness parameters, for accuracy, and as a result it may have to operate very close to the minimum time step τ_{NE}.

References

[1] Wichaidit C and Hitchon W N G 2005 *Phys. Lett.* A **335** 50
[2] Dhali S K and Williams P F 1985 *Phys. Rev.* A **31** 1219
[3] Yoshida K and Tagashira H 1976 *J. Phys. D: Appl. Phys.* **9** 485
[4] Wu C and Kunhardt E E 1988 *Phys. Rev.* A **37** 4396
[5] Kulikovsky A A 1994 *J. Phys. D: Appl. Phys.* **27** 2556
[6] Boeuf J P 1988 *J. Appl. Phys.* **63** 1342
[7] Li J and Dhali S K 1997 *J. Appl. Phys.* **82** 4205
[8] Barnes M S, Colter T J and Elta M E 1987 *J. Appl. Phys.* **61** 81
[9] Aleksandrov N L and Bazelyan E M 1996 *J. Phys. D: Appl. Phys.* **29** 740
[10] Guo J M and Wu C J 1993 *J. Phys. D: Appl. Phys.* **26** 487
[11] Guo J M and Wu C J 1993 *IEEE Trans. Plasma Sci.* **21** 684
[12] Carman R J and Mildren R P 2003 *J. Phys. D: Appl. Phys.* **36** 19
[13] Carman R J and Mildren R P 2002 *IEEE Trans. Plasma Sci.* **30** 154
[14] Kanzari Z, Yousfi M and Hamani A 1998 *J. Appl. Phys* **84** 4161
[15] Oh Y H, Choi N K and Choi D I 1990 *J. Appl. Phys.* **67** 3264
[16] Passchier J D P and Goedheer W J 1993 *J. Appl. Phys.* **74** 3744
[17] Wichaidit C and Hitchon W N G 2005 *J. Comput. Phys.* **203** 650
[18] Hitchon W N G 1999 *Plasma Processes for Semiconductor Fabrication* (Cambridge: Cambridge University Press)
[19] Wichaidit C and Hitchon W N G 2004 *J. Phys. D: Appl. Phys.* **37** 2545
[20] Nadis G V 1997 *Tech. Phys. Lett.* **23** 493
[21] Penny G W and Hummert G T 1970 *J. Appl. Phys.* **41** 572
[22] Morrow R and Blackburn T R 1999 *IEEE Trans. Plasma Sci.* **27** 26
[23] Kulikovsky A A 2000 *J. Phys. D: Appl. Phys.* **33** 1514
[24] Pancheshnyi S V, Starikovskaia S M and Yu Starikovskii A 2001 *J. Phys. D: Appl. Phys.* **34** 105
[25] Christlieb A J, Krasny R and Verboncoeur J P 2004 *IEEE Trans. Plasma Sci.* **32** 384
[26] Eastwood J W 1986 *Comput. Phys. Commun.* **43** 89
[27] Eastwood J W 1987 *Comput. Phys. Commun.* **44** 73
[28] Purser R J and Leslie L M 1994 *Mon. Weather Rev.* **122** 745
[29] Feng J and Hitchon W N G 2000 *Phys. Rev.* E **61** 3160
[30] Sommerer T J, Hitchon W N G and Lawler J E 1989 *Phys. Rev.* A **39** 6356
[31] Christlieb A J, Hitchon W N G and Keiter E R 2000 *IEEE Trans. Plasma Sci.* **28** 2214